

Results and Prospects of Few-Body System Structure Studies

Eric Voutier

*Laboratoire de Physique Subatomique et de Cosmologie
IN2P3-CNRS/Université Joseph Fourier
53 avenue des Martyrs
38026 Grenoble cedex, France*

*Thomas Jefferson National Accelerator Facility,
12000 Jefferson avenue
Newport News, Virginia 23606, USA*

Abstract

This paper presents a selected review of the $(e, e'p)$ experimental program recently completed at the Jefferson Laboratory in the domain of high momentum transfer and high recoil momentum. Particular emphasis is put on the current understanding of the reaction mechanisms and of the large final state interaction effects. Their consequences on the study of the nuclear wave function and nucleon-nucleon correlations are addressed. The short and long term future of the $(e, e'p)$ experimental program is also discussed in the perspective of the study of the quark and gluon structure of nucleons and nuclei.

1 Introduction

Since the very first experiments at Frascati, Saclay, and NIKHEF the $(e, e'p)$ reaction has been proven a powerful tool for the investigation of nuclear structure [1,2]. The advent of high energy electron beams with high intensity and duty cycle has opened access to the high momentum range, a region expected to reveal peculiar features of the nucleon substructure. Indeed, large virtual photon momentum q allows access to distances scales $\sim \hbar/q$ that are comparable or smaller than the nucleon radius. In addition, the $(e, e'p)$ Meson Exchange Current (MEC) mechanism at large q is expected to be less important due to the natural decrease built into the meson propagators and form factors. Therefore, one can expect to probe more reliably high initial momenta in the nucleus, that is small inter-nucleon distances, and learn about

the origin of the short-range repulsion of the NN interaction from its standard representation up to the most exotic descriptions.

The general framework of nuclear structure studies has been evolving since the first generation of $(e, e'p)$ experiments at the Continuous Electron Beam Accelerator Facility (CEBAF) of the Jefferson Laboratory (JLab). This paper reviews our present understanding of the dynamics of the $(e, e'p)$ reaction. Particularly, the dominance of the Final State Interactions (FSI) and its consequences for the study of the nucleon and nuclear structure are discussed. Future prospects in this domain as well as more exotic use of the $(e, e'p)$ reaction in the study of the Color Transparency (CT) phenomenon are also addressed.

The next section introduces the basic concept and description of the $(e, e'p)$ reaction. Recent results on D [3], ^3He [4], and ^4He [5] are then discussed which allow one to envisage more sensitive investigations of the CT phenomenon [6]. The problem of the left-right asymmetry observable is then discussed on the basis of a comparison between few- and many-body experimental results [4,7]. In sec. 6, the most recent investigations of nucleon-nucleon correlations [8,9] in the nuclear medium are presented. Finally, the long standing issue of bound nucleon form factors is revisited in light of the new JLab measurements [10].

2 The $(e, e'p)$ Reaction

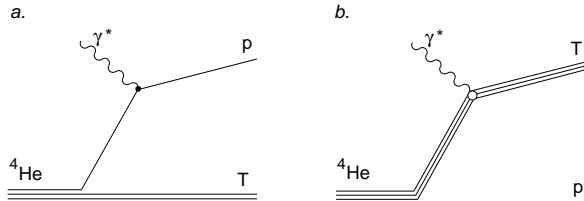


Figure 1. One-body contributions to the $^4\text{He}(e, e'p)$ reaction: plane wave impulse approximation (a), and recoil contribution (b).

The merit of quasi-elastic electron scattering for the study of nuclear structure is in the description of the reaction process in the framework of the Plane Wave Impulse Approximation (PWIA). In this context (fig. 1a), the cross section for the $(e, e'p)$ process can be factorized in two terms: one representing the probability of a virtual photon to interact with a proton, that is the electron-bound proton cross section σ_{ep} [11], and another representing the probability to find a proton in the nucleus with initial momentum \vec{p}_m and binding energy E_m , that is the nuclear spectral function $S(p_m, E_m)$ [1,2]. Tagging the virtual photon $(\vec{q}, \omega) = (\vec{k} - \vec{k}', E - E')$ by measuring the four-momenta (\vec{k}, E) and (\vec{k}', E') of the incoming and scattered electron, and measuring the four-momentum (\vec{p}, E_p) of the knocked-out proton, one reconstructs

$$\vec{p}_r = \vec{q} - \vec{p} \quad (1)$$

$$E_m = \omega - T_p - T_r . \quad (2)$$

Within PWIA, the momentum \vec{p}_r of the recoil system is equal to the opposite of the initial momentum \vec{p}_m of the proton. Then, studying the dependence of the cross section either on (q, ω) or on (p_m, E_m) , one can access directly different features of the nuclear structure. Particularly, at high initial momentum, one can determine the importance and the origin of high momentum components of the nuclear wave function, test the existence of relativistic effects or learn about short range correlations. At high momentum transfer, one can question the validity of the current operator or investigate the electromagnetic properties of bound nucleons, and possible exotic configurations.

However, depending on the kinematics of the reaction, several other mechanisms interfere with the elementary PWIA amplitude. FSI, where the knocked-out proton interacts with the residual nucleus (fig. 2) distort the nuclear information and break the simple factorization scheme of the cross section. In addition, instead of interacting with nucleons, the photon can couple to the virtual mesons of the nuclear field leading to a large variety of MEC contributions (fig. 2).

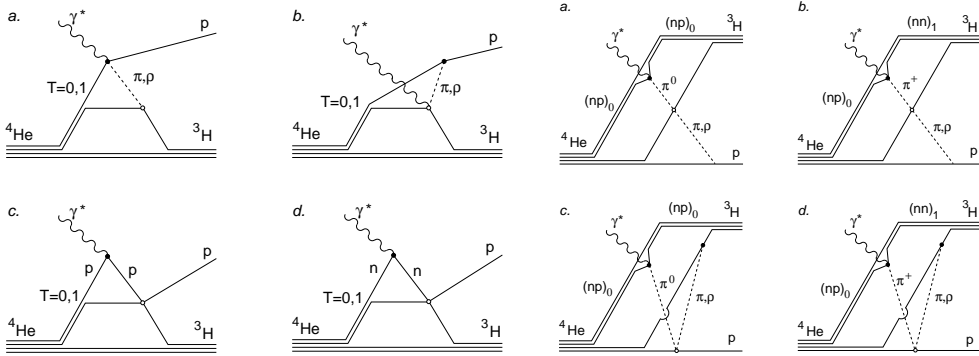


Figure 2. Two-body (four left diagrams) and three-body (four right diagrams) contributions to the ${}^4\text{He}(e, e'p)$ reaction: final state interaction (c and d of left panel), and meson exchange currents (all other diagrams).

One way to disentangle the different reaction mechanisms and select the PWIA amplitude is to separate the elementary components or response functions of the cross section and to take advantage of peculiar kinematics conditions. For instance, MEC essentially affect the transverse components of the hadronic current and their effects are expected to decrease at high momentum transfers because of the natural Q^{-2} evolution of meson form factors.

The unpolarized cross section for the $A(e, e'p)$ process may be written

$$\frac{d^6\sigma}{dk'd\vec{p}} = |\vec{p}| E_p \sigma_M \left[V_L R_L + V_T R_T + V_{LT} R_{LT} \cos(\phi) + V_{TT} R_{TT} \cos(2\phi) \right] \quad (3)$$

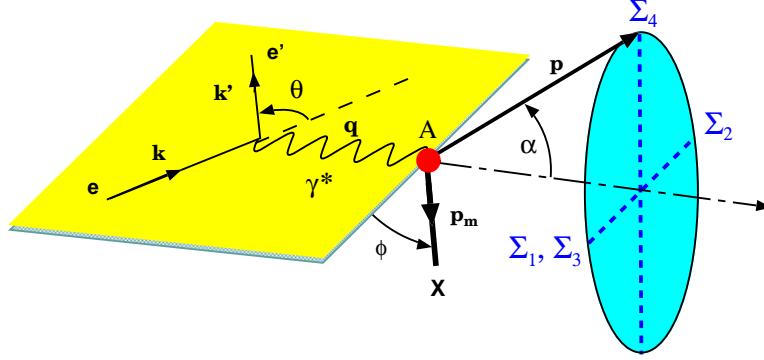


Figure 3. The leptonic and hadronic planes for the $(e, e'p)$ process.

where σ_M is the Mott cross section for a structureless nucleus

$$\sigma_M = \alpha^2 \left(\frac{1}{2E \sin(\theta/2)} \right)^2 \tan^2 \left(\frac{\theta}{2} \right) \quad (4)$$

with θ the electron scattering angle and ϕ the angle between the leptonic and hadronic planes (fig. 3). The V_i are the kinematical factors

$$V_L = \frac{Q^4}{q^4} \quad (5)$$

$$V_T = \frac{1}{2} \frac{Q^2}{q^2} + \tan^2 \left(\frac{\theta}{2} \right) \quad (6)$$

$$V_{TT} = \frac{1}{2} \frac{Q^2}{q^2} \quad (7)$$

$$V_{LT} = \frac{Q^2}{q^2} \left[\frac{Q^2}{q^2} + \tan^2 \left(\frac{\theta}{2} \right) \right]^{1/2} \quad (8)$$

depending on the virtual photon four-momentum characteristics; Q^2 the relativistic invariant $q^2 - \omega^2$, by convention. The R_i represent the response of the nuclear system to the electromagnetic excitation and can be expressed as

$$R_L = \rho \rho^\dagger \quad (9)$$

$$R_T = J_x J_x^\dagger + J_y J_y^\dagger \quad (10)$$

$$R_{TT} \cos(2\phi) = J_x J_x^\dagger - J_y J_y^\dagger \quad (11)$$

$$R_{LT} \cos(\phi) = -(\rho J_x^\dagger + J_x \rho^\dagger) \quad (12)$$

in terms of the hadronic current (\vec{J}, ρ) in the reference frame of the virtual photon (fig. 3). The separation of these four response functions requires four different measurements (Σ_i on fig. 3): measuring the cross section on the right

(Σ_1) and left (Σ_2) of the virtual photon at constant (\vec{q}, ω) and (\vec{p}, E_p) , one extracts the longitudinal-transverse interference response R_{LT} ; an additional measurement out of the reaction plane (Σ_4) allows one to obtain the transverse-transverse interference response R_{TT} ; a last measurement at a different beam energy (Σ_3) allows one to separate the longitudinal R_L and transverse R_T responses by changing the electron scattering angle.

Following this philosophy, several $(e, e'p)$ experiments on few-body systems at high momentum transfer and high recoil momentum have been completed using the High Resolution Spectrometers [12] of the hall A of JLab. Few-body systems are indeed privileged laboratories since exact microscopic calculations can be achieved involving the full complexity of the NN interaction.

3 High Momenta Cross Sections

Beyond the experimental benefit of the large duty factor of CEBAF, the several GeV beam energy allows one to access very small cross sections typical of the high recoil momentum region. Therefore, the cross section can be mapped over a large range of recoil momentum without changing the virtual photon probe. This feature is an important improvement with respect to older experiments at smaller scale facilities: keeping the leptonic vertex constant gives a better handling of the reaction mechanisms and consequently insures a better interpretation of experimental data.

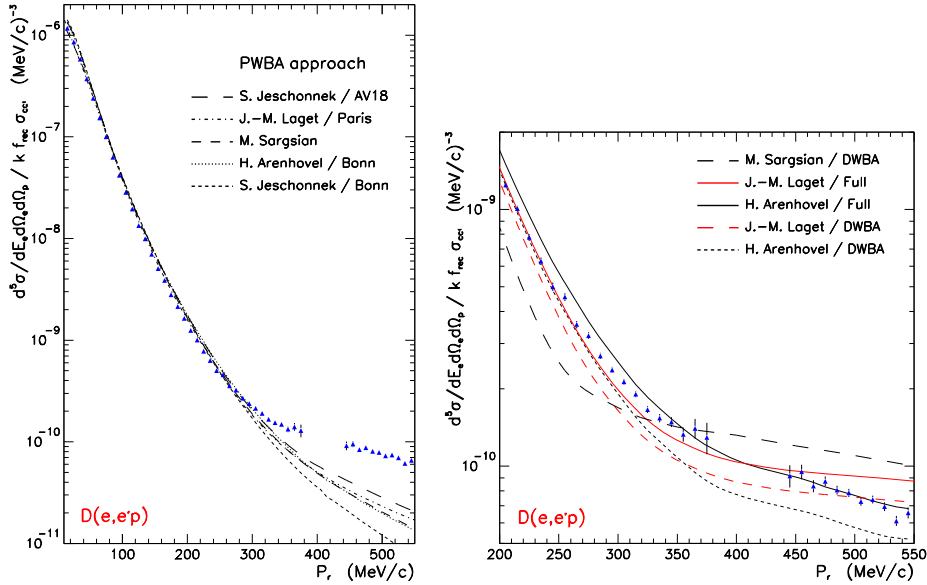


Figure 4. Experimental data of the E94-004 experiment [3]: comparison to PWIA calculations (left) over the full range of measured p_r , and comparison to full calculations (right) in the high momentum region

3.1 $D(e, e'p)$ cross section

The first experiment reported here is about deuterium, the elementary laboratory nucleus of the NN interaction. This $D(e, e'p)$ electro-disintegration experiment [13] has been performed in quasi-elastic kinematics at $Q^2 = 0.67 \text{ GeV}^2$ and $x = Q^2/2M_p\omega = 0.96$. The recoil neutron is reconstructed (eq. 1) perpendicular to the virtual photon. Experimental data are compared in fig. 4 to several calculations. It is particularly shown that all PWIA calculations using different methods and/or nuclear wave functions fail to reproduce the data at large recoil momentum. Above 300 MeV/c, FSI drive the cross section and small but still active MEC have to be taken into account as shown by calculations from H. Arenhövel [3] and J.-M. Laget [14].

3.2 ${}^3\text{He}(e, e'p)$ cross section

Because of its higher density, the helium nucleus is expected to reveal more fine details of the NN interaction. It is also a bridge between few- and many-body systems where one can investigate the strength of three-body forces.

A selected set of data from the ${}^3\text{He}(e, e'p)d$ JLab experiment [15] is shown in fig. 5. The experiment was performed in perpendicular kinematics at constant $Q^2 = 1.52 \text{ GeV}^2$ and $x = 0.99$, reaching for the very first time the 1 GeV/c recoil momentum range. It corresponds to an unprecedented measurement of the cross section over six orders of magnitude.

The top left panel of fig. 5 represents the reduced cross section for the three beam energies of the experiment as compared to older results [16,17] and a PWIA calculation [18]; within PWIA, the reduced cross section corresponds to the nuclear spectral function $S(|\vec{p}_m| = |\vec{p}_r|, E_m = 5.4 \text{ MeV})$. Good agreement with older data is obtained up to 250 MeV/c. Above this value, data dispersion is observed corresponding, for different beam energies, to different magnitude of the reaction mechanisms beyond PWIA. This is confirmed by the comparison to a PWIA calculation where the agreement degrades gradually starting about 100 MeV/c.

Similarly to the deuterium case, the high momentum range (fig. 5 bottom panel) exhibits strong effects from the interaction of the knocked-out proton with the residual system: below 300 MeV/c, the PWIA cross section is moderately quenched while above this value strong enhancement of the cross section (about a factor 5 at 500 MeV/c) is observed. Different calculations [19,20] confirm that FSI is the driving contribution, MEC being quasi-negligible, as expected in this Q^2 range. Note that, presented at this workshp, new calculations [21] within a Relativistic Distorted Wave Impulse Approximation (RDWIA) show good agreement with data and lead to the same conclusion

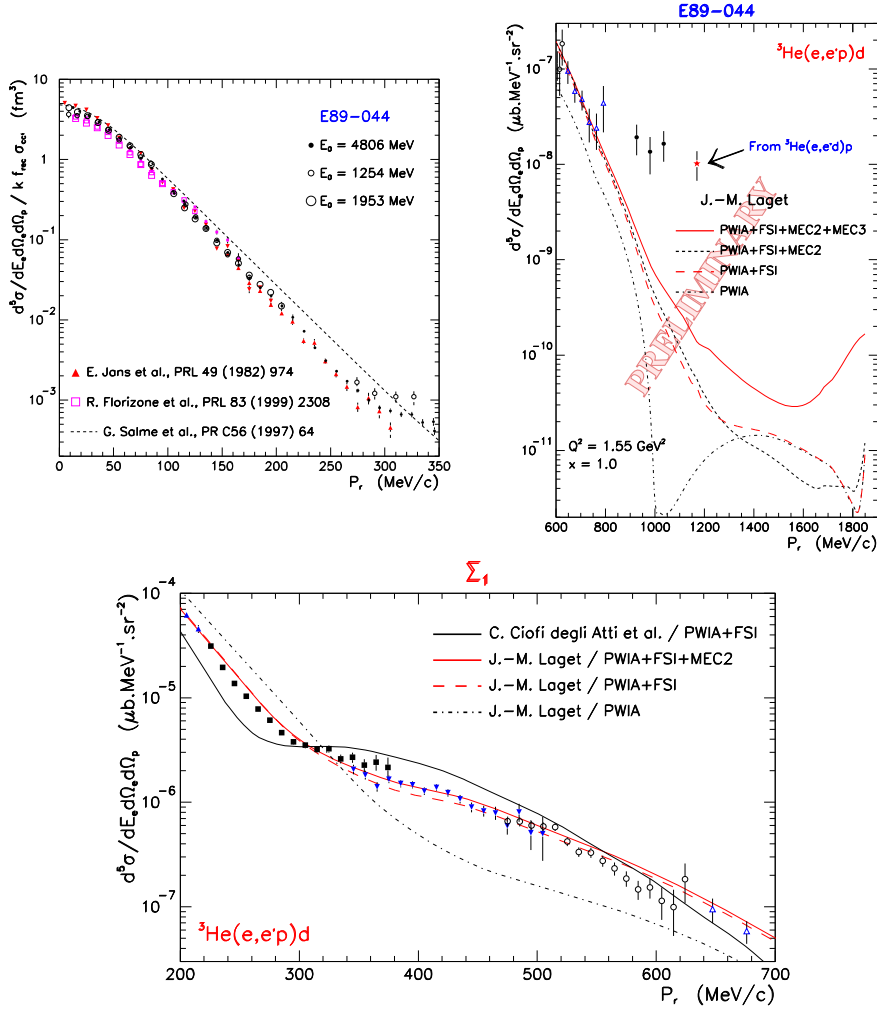


Figure 5. Selected data of the E89-044 experiment [4]: comparison to previous experiments (top left), comparison to model calculations in the high (bottom) and very high (top right) recoil momentum region.

about the dominance of FSI in this energy range.

In the very high momentum region (fig. 5 top right), which was explored for the very first time, the cross section seems to saturate at an unexpectedly high level. These data are confirmed by the measurement of the recoil deuteron in the same experiment [22]: within a simple jacobian transformation, the ${}^3\text{He}(e, e'p)d$ cross section is deduced from the measured ${}^3\text{He}(e, e'd)p$ cross section. Calculations are unable to reproduce this excess of strength at 1 GeV/c. Whether it is a consequence of the truncation of the diagrammatic expansion [14] or a signature of other degrees of freedom is an open question. More data on this experiment are available in [23], particularly a separation of the response functions was achieved which however does not bring additional information on the nuclear structure due to the magnitude of FSI effects.

3.3 ${}^4\text{He}(e, e'p)$ cross section

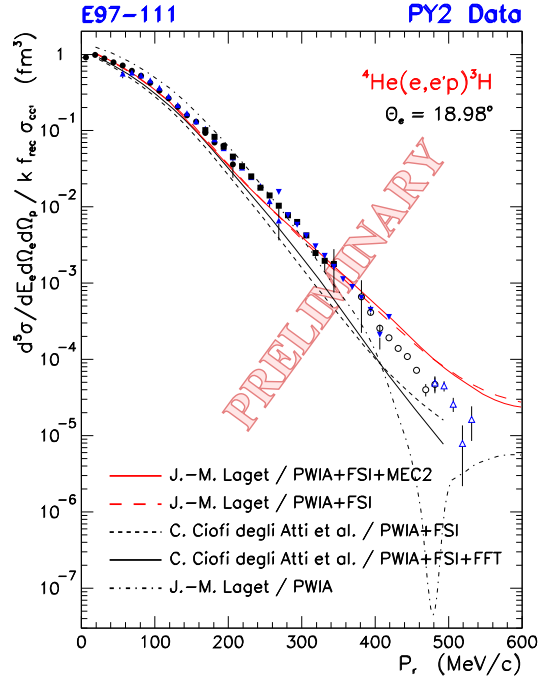


Figure 6. Selected preliminary data of the E97-111 experiment [5] measured for a 3.170 GeV beam energy and a fixed electron scattering angle $\theta_e = 18.98^\circ$: the different curves are several model calculations.

Another attempt to pin down the nuclear wave function at high recoil momentum was investigated in a ${}^4\text{He}(e, e'p){}^3\text{H}$ experiment [24]. It was shown by S. Tadokoro et al. [25] that this nucleus is particularly sensitive to the details of the short range part of the NN interaction: within an independent particle approach, computing the spectral function from a realistic potential, they found that it shows a typical diffractive pattern which minima position and height are sensitive to the fine structure of the NN interaction. The expected position at about 450 MeV/c lies in the high momentum range and it is not surprising that a previous experiment at smaller beam energy [26] was unable to observe it, suffering from large FSI and MEC effects that fill the dip.

The E97-111 experiment took data in parallel kinematics which is expected to minimize FSI. Here, the knocked-out proton and the recoil system are emitted along the direction of the virtual photon. Because data were taken at constant beam energy and scattered electron angle, the momentum evolution of the cross section mixed different (\vec{q}, ω) , as opposed to the previously reported experiment. Experimental data are compared to theoretical calculations in fig. 6: they all show large FSI effects which forbid observation of the minimum.

In conclusion, these experiments, which are relatively well understood by theoretical calculations using modern nuclear wave functions, show the dominance

of FSI at high recoil momentum. These large effects consequently forbid us to go beyond the actual knowledge of the NN interaction and learn about the fine details of the wave function. There are however theoretical expectations and experimental indications [5,27] that at large x , when the direction of the initial proton momentum is opposed that of the virtual photon, the magnitude of FSI should decrease, enabling the selection of the PWIA amplitude.

4 Final State Interactions and Color Transparency

The main process at work in the interaction of the knocked-out proton with the residual system is the NN scattering. Because of the large energy transfer in JLab experiments, the proton can rescatter on a nucleon at rest which then gains momentum and is emitted at about 90° with respect to the proton. In this way, part of the strength at small initial momentum is shifted towards high recoil momentum. FSI are then maximal at large p_r in perpendicular kinematics. More strictly, the position of this maximum corresponds to the singularity of the nucleon propagator which occurs at $x = 1$ in the $(e, e'p)$ channel [14]: the electron scatters on a proton which propagates on-shell in the nuclear medium and rescatters on a nucleon at rest. Since the PWIA amplitude falls rapidly with p_r , the on-shell rescattering takes over and dominates at large p_r .

Several theoretical treatments of FSI exist in the literature ranging from microscopic to macroscopic approaches: in the diagrammatic approach of J.-M. Laget, FSI are parametrized in terms on the NN partial wave expansion for $\omega < 500$ MeV, and in terms of a high energy parametrization fitted to the NN scattering world data at larger excitation energy [14]; Glauber based calculations are also available [20,30] as well as a Generalized Eikonal Approximation [31] that takes into account the Fermi motion of the target nucleon, as opposed to Glauber; optical potential approaches have also been developed [21].

This important theoretical activity as well as the still open question of the origin of the high momentum components of the wave function has motivated a systematic study of the $(e, e'p)$ reaction in the elementary deuterium nucleus. The E01-020 experiment [28] has measured the angular distribution of the recoil neutron (or x distribution ¹) in the $D(e, e'p)$ reaction over the complete allowed phase space at fixed Q^2 and p_r . Preliminary data [29] at $Q^2 = 2.1$ GeV² and several recoil momenta are reported in fig. 7 in terms of the ratio of the measured experimental cross section to a model calculation of the PWIA amplitude. A point-to-point comparison to theoretical calculations should not

¹ At fixed Q^2 and p_r , the angle of the recoil particle and the x variable are linked via a unique relationship, large x corresponding to small recoil angles.

be attempted here because of the very preliminary stage of the analysis, only the general shape and behaviour of the data is relevant. The general trend of data is in agreement with calculations, showing a moderate FSI quenching of the cross section at small p_r and an impressive FSI enhancement at large p_r . At 400 MeV/c recoil momentum, the peak position is shifted below $x = 1$ which, similarly to the on-shell nucleon mechanism, corresponds to the propagation of an on-shell Δ resonance in the nuclear medium.

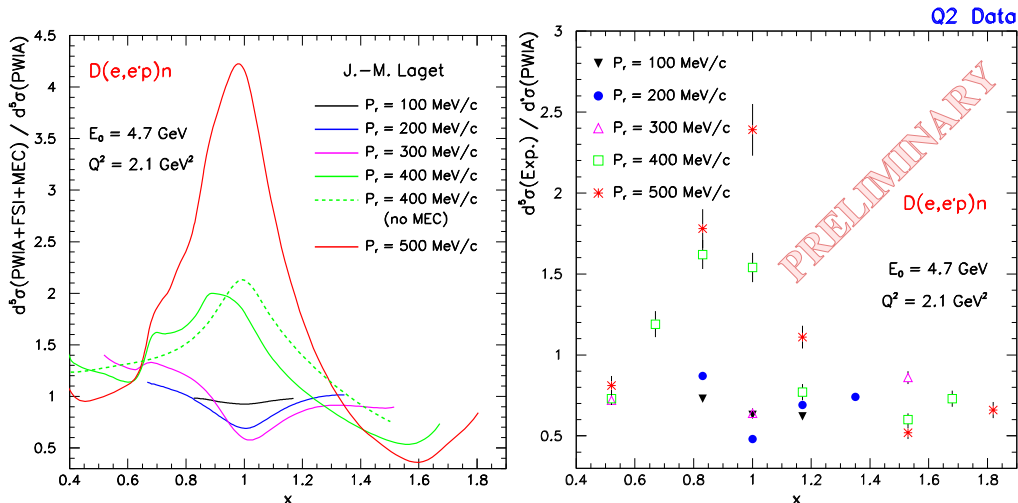


Figure 7. Selected preliminary data (right panel) of the E01-020 experiment [29] at $Q^2 = 2.1$ GeV² and several recoil momenta, together with corresponding theoretical calculations [14] (left panel).

This simple on-shell rescattering mechanism which relies on elementary on-shell amplitudes opens an original use of the $(e, e'p)$ reaction, namely, the study of the CT phenomom in few-body systems [32,33].

Color Transparency is a direct consequence of Quantum Chromo-Dynamics that predicts the existence, in the nucleon wave function, of a minimal valence state where the quarks are very close together and constitute a small size color neutral object (or mini-hadron). Such a color singlet system cannot emit or absorb soft gluons and therefore experiences much reduced strong interaction with other nucleons when travelling through the nuclear medium.

The experimental evidence of CT not only requires the selection of a small size configuration but also a clear signature of the subsequent reduced interaction. As of now, the several experimental attempts [34,35,36] to search for CT in many-body systems have failed. The common understanding is that the coherence length, that is the distance needed for the mini-hadron to evolve from its minimal valence state toward its asymptotic wave function, is too small with respect to the typical nuclear scale.

Few-body systems may solve this problem by taking advantage of the dominance of FSI in perpendicular quasi-elastic kinematics: the signature of CT would appear as a decrease of the cross section at $x = 1$ as a function of Q^2 ,

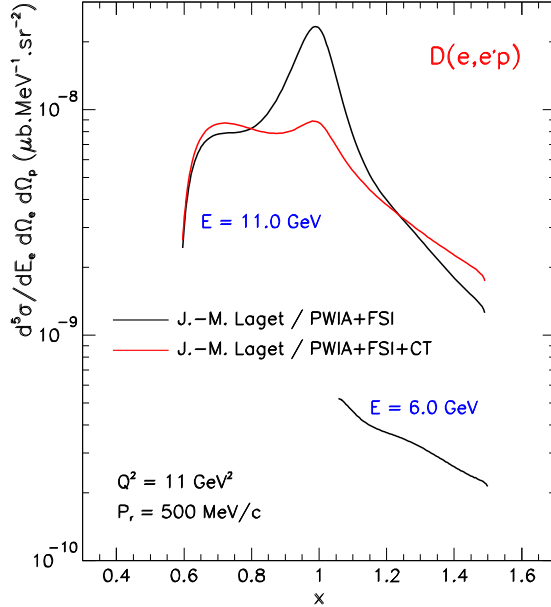


Figure 8. Predictions for the x distribution of the $D(e, e'p)$ cross section at fixed $Q^2 = 11 \text{ GeV}^2$ and $p_r = 500 \text{ MeV}/c$ for two different beam energies: CT effects (red curve) result in a reduction of the cross section at $x = 1$.

due to the gradual suppression of FSI with diminishing mini-hadron size. A similar example is shown on fig. 8 in the context of the 12 GeV upgrade project at JLab [6]. The merits of the energy upgrade to access a wide x range at large Q^2 is obvious. This particularly allows the study of the $D(e, e'p)$ reaction in the quasi-elastic region where the existence of CT would lead to large effects on the cross section.

5 The A_{LT} Dilemma

As explained in sec. 2, the study of $(e, e'p)$ reactions at JLab is not restricted to cross section measurements. Some experiments aimed at and achieved a separation of the response functions [7,23]. Particularly, the longitudinal-transverse interference response was extracted. From the same data, one can also reconstruct the A_{LT} observable (see fig. 3)

$$A_{LT} = \frac{\Sigma_2 - \Sigma_1}{\Sigma_2 + \Sigma_1} = \frac{V_{LT}R_{LT}}{V_{LR}R_L + V_{TR}R_T + V_{TT}R_{TT}} \quad (13)$$

which corresponds to the left-right asymmetry with respect to the virtual photon. This observable downplays the significance of the ground-state wave function by virtue of the ratio involved in its definition [2]. There exists indications that it is sensitive to relativistic effects at small momentum ($p_r < 200 \text{ MeV}/c$) [37], and more generally to any mechanism that breaks the simple

factorization scheme of the cross section [38].

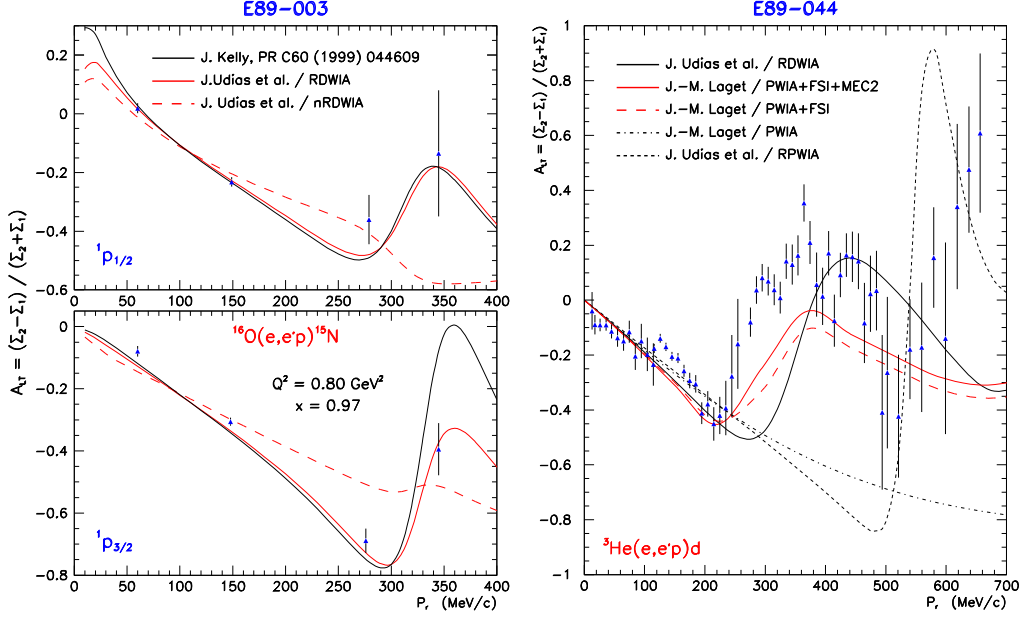


Figure 9. Left-right asymmetry measurements in the ^{16}O [7] (left panel) and ^3He [4] (right panel) nuclei: the curves show different calculations as explained in the text

Figure 9 shows the experimental data for this observable measured in the E89-003 [39] and E89-044 [15] experiments for the ^{16}O and ^3He nuclei, respectively. A_{LT} shows a typical oscillating pattern characteristic from factorization breakdown which originates however from quite different mechanisms in each case. In the ^{16}O case, different calculations [40,41,42] show that the oscillation comes from relativistic corrections to the proton wave function via the enhancement of lower spinor components [38]. In the ^3He case, FSI are responsible for this behaviour [14,21] which occurs at a similar recoil momentum. It is instructive to compare on the right panel of fig. 9 the microscopic (J.-M. Laget) and mean field approach (J. Udias *et al.*) calculations. An important feature of the relativistic calculation is the breakdown of the cross section factorization at the PWIA level [38] which generates the large oscillation seen at high recoil momentum. This feature is not reproduced by the microscopic approach which has a smooth variation in PWIA. When taking into account FSI within two different methods – optical potential for the many-body approach and high energy parametrization of the NN scattering for the microscopic one – both calculations get similar agreement with data. This not only confirms the importance of FSI but also the relative insensitivity of A_{LT} to the nuclear wave function, and would suggest that this observable is more sensitive to the elementary current operator. There are no microscopic calculations for ^{16}O but the difference between distorted non-relativistic and relativistic calculations clearly signifies the importance of relativistic corrections to the wave function. It is still a mystery how the same observable can be sensitive or insensitive to the wave function depending on the nucleus.

The decrease of the nuclear density when going from ^{16}O to ^3He has been proposed to explain the suppression of relativistic effects [21]. The E01-108 experiment [43] will study the $(e, e'p)$ reaction in ^4He for kinematical conditions similar to the ^3He experiment [15] investigating, among other observables, A_{LT} . The higher density of the ^4He nucleus will allow this feature to be tested and make a bridge between many-body and few-body approaches.

6 Nucleon-Nucleon Correlations

The search for NN correlations with the $(e, e'N)$ and $(e, e'NN)$ reactions is also an important topic of the JLab experimental program. At high recoil momentum, one expects to learn about the short-range repulsive part of the NN interaction, and at some point, to abandon the traditional mesonic description of the nuclear field in favor of a smaller scale description involving the quark substructure of the nucleon.

6.1 $(e, e'p)$ channel

One possible experimental method to study this issue is to select a correlated pair in the nucleus and measure the recoil momentum distribution [44]. In PWIA, the residual system does not participate in the reaction and consequently, the p_r distribution directly reflects the initial momentum distribution. Within this context the selection of a correlated pair in a $A(e, e'p)$ experiment is insured by a strict kinematical relationship between E_m and p_r

$$E_m = \sqrt{\left(M_{A-2} + \sqrt{M_N^2 + p_r^2}\right)^2 - p_r^2} + M_p - M_A \quad (14)$$

where the M_i are the nucleons and nuclei mass involved in the process. Thus, in PWIA, a signature of the disintegration of a correlated pair is the appearance of a peak in the cross section as a function of E_m , in the continuum region, which position depends on p_r .

This experimental method was applied in the E89-044 experiment [15] at JLab which has investigated the $^3\text{He}(e, e'p)np$ electro-disintegration of the ^3He nucleus in the continuum region. Data taking was performed in perpendicular kinematics up to 1 GeV/c, at constant electron momentum and angle allowing for a better control of the hadronic current. In addition, as compared to previous experiments [17,44], the E_m acceptance of the JLab experiment is large enough to investigate the pair momentum distribution without suffering from

truncation and subsequent extrapolation of the spectra of the relative energy of the pair [45].

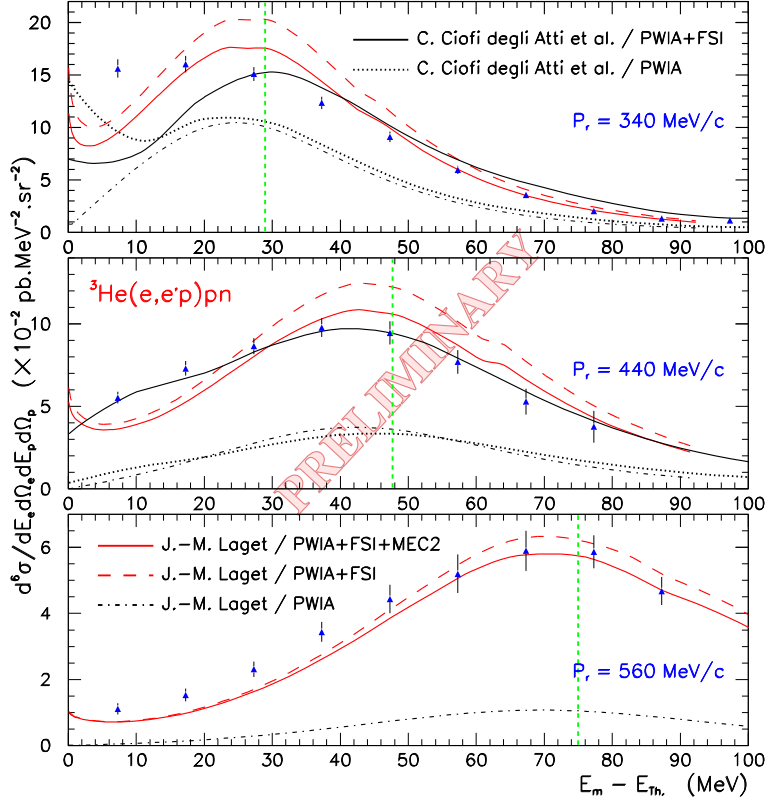


Figure 10. Selected data of the E89-044 experiment in the continuum region [9]: the green vertical line indicates the expected location of the correlated pair peak; calculations are from C. Ciofi degli Atti [20] and J.-M. Laget [14] for different model approximations.

The experimental missing energy distribution for selected recoil momenta is compared in fig. 10 to different calculations. A broad peak is observed at about the expected location, supporting the observation of a correlated pair in ${}^3\text{He}$. However, calculations clearly show that the measured strength can only be explained by large FSI contributions and a significant MEC correction at small recoil momentum. It originates mainly from the re-interaction in the pair and to a lesser extent from the re-interaction with the residual nucleon. Therefore, as in the two-body disintegration case (sec. 3.2), it is not possible to extract an exact value of the actual pair momentum distribution because of the small contribution of the PWIA amplitude to the reaction cross section. In fact, the relationship of eq. 14 is valid as long as the reaction involves two active nucleons with a spectator residual system. When the nucleon of the active pair rescatters, the position, the width and the shape of the peak might all be affected, the FSI dominance in the pair being consistent with previous observations (sec. 3.1).

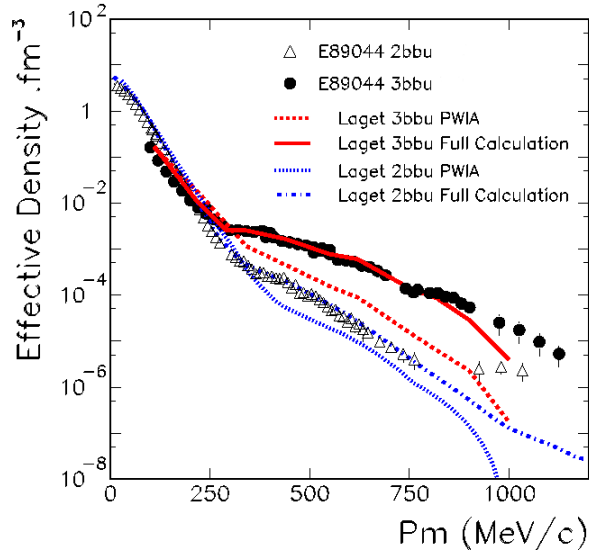


Figure 11. Effective nucleon momentum distributions in ${}^3\text{He}$: experimental results for the two- [23] and three-body [45] breakup are compared to calculations from J.M.-Laget [14].

In the absence of factorization of the cross section, one can reconstruct the effective momentum distribution (also known as the reduced cross section in the literature), extracted from data by removing the electron dependent part. In the particular case of the E89-044 experiment, the two-body and three-body breakup channels were simultaneously measured, at the same electron kinematics. Therefore, the comparison between the two effective momentum distributions tells about the nuclear structure. Fig. 11 particularly suggests that high momentum configurations preferably originate from correlated pairs in the nucleus. Using modern potentials and nuclear wave functions, theoretical calculations are in good agreement with data, and confirm the important role of short-range correlations.

6.2 $(e, e'pN)$ channel

While $(e, e'p)$ reactions lead as today to indirect evidence of short-range correlations, there are expectations that two-body knockout reactions would provide direct and sensitive measurements. To date, the few achieved experiments in many- and few-body systems [46,47,48] still show strong sensitivity to competing reaction mechanisms involving FSI, MEC and Δ excitation (see [49] for more details).

The E89-027 experiment [50] in hall B of JLab takes advantage of the large

phase space coverage of CLAS (CEBAF Large Acceptance Spectrometer) [51] to study the ${}^3\text{He}(e, e'pN)$ reaction over a wide range of energy and momentum transfers. By selecting all nucleon momenta above the Fermi momentum and restricting the perpendicular component (transverse to \vec{q}) of the fast nucleon to below 300 MeV/c, the emphasis is put on configurations where the virtual photon interacts with the leading nucleon while the associated correlated pair stays at rest [8]. For such configurations, different calculations show that FSI and two-body currents of the leading nucleon are suppressed but the continuum state interactions of the spectator pair and three-body exchange currents play an important role, distorting the elementary nuclear information.

In the near future, with the help of the newly built Big Bite spectrometer [52], NN correlations will be investigated in carbon [53] for anti-parallel kinematics where the PWIA amplitude is expected to be dominant.

7 Bound Nucleon Form Factors

There are many reasons to at least question the electromagnetic properties of bound nucleons as compared to free ones: within the nuclear field, the nucleon mass changes from its free value to an effective value depending on the intensity of the binding force; the bound Dirac spinors describing nucleons differ from free ones, the enhancement of the lower spinor components being the basic effect of relativistic corrections in A_{LT} [38]; there are three different prescriptions for the current operator which are equivalent for on-shell nucleons only, and which would strictly lead to twelve different form factors for bound nucleons instead of the two usual Dirac and Pauli form factors [2]... Unfortunately, the determination of the modifications of nucleon properties can only be done within a model: nucleon changes like the polarization of the surrounding meson cloud or the excitation of the quark hard core are intertwined with conventional MEC and isobar currents.

An experimental method to minimize these effects and get closer to the in-medium nucleon information is the measurement of polarization transfer observables [54,55] in quasi-elastic scattering of longitudinally polarized electrons. In the free proton case, one can write

$$\frac{G_E}{G_M} = -\frac{P_t}{P_l} \frac{E + E'}{2M_p} \tan\left(\frac{\theta}{2}\right) \quad (15)$$

where P_t and P_l are the measured transverse and longitudinal components of the proton polarization. This method was successfully applied in the measurement of the electric form factor of the free proton [56,57], one of the most important experimental result of the decade which points to the existence of quark orbital momentum. Thanks to these data, the possible existence of

two photon exchange contributions [58] strongly questions cross section measurements to access the nucleon form factors at high Q^2 . In addition, the polarization transfer method is supposed to be intrinsically less sensitive to many-body effects.

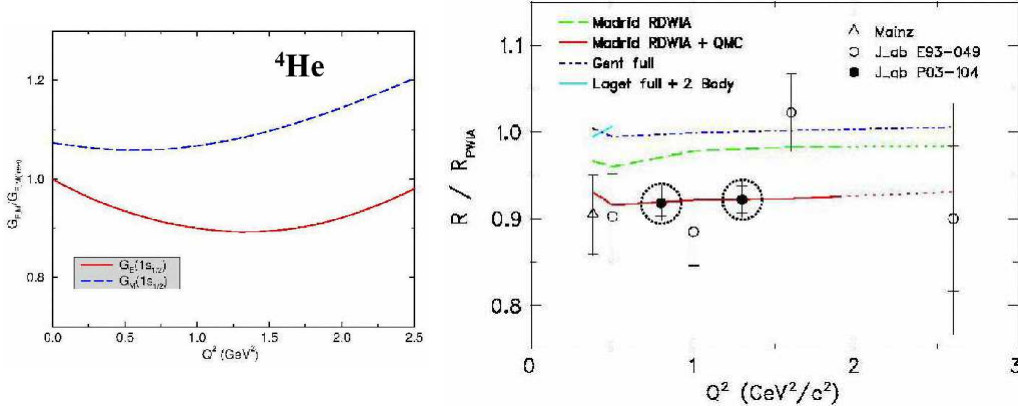


Figure 12. The modification of in-medium proton form factors: theoretical expectations in ${}^4\text{He}$ [61] (left panel), and measured [10] and projected [62] experimental results (right panel). The latter are expressed in terms of the ratio of the measured polarization ratio $R = (P_t/P_l)_{4\text{He}}/(P_t/P_l)_\text{H}$ normalized by the free value, to the same ratio calculated in PWIA.

Following a previous measurement at small Q^2 in MAMI [59], the JLab E93-049 experiment [60] had investigated this problem in the ${}^4\text{He}(\vec{e}, e'\vec{p}){}^3\text{H}$ quasi-elastic scattering where theoretical calculations predict a sizeable change of the proton electromagnetic form factors, originating mainly from the enhancement of the lower spinor components of the in-medium quark wave function [61]. Experimental data [10] are shown in fig. 12 together with several calculations. The most modern calculations considering free form factors and many-body dynamics fail to reproduce data. Agreement is only obtained after including in these calculations the predicted modifications [61]. The authors [10] claim for an evidence of medium modifications. However, the accuracy of the data does not yet allow a definitive conclusion. It is the purpose of the E03-104 experiment [62] to provide high accuracy data (fig. 12) in this momentum range and hopefully confirm this finding.

8 Conclusions

To date, the $(e, e'p)$ JLab experimental program on few-body systems has established the dominance of FSI on top of the quasi-elastic peak. FSI are responsible for moderate quenching ($p_r < 300$ MeV/ c) and large enhancement ($p_r > 300$ MeV/ c) of the cross section, and result in a large oscillation in A_{LT} . The same mechanism also obscures the signal from correlated nucleon pairs.

This all confirms that the high momentum components of the nuclear wave function cannot be measured in such kinematics, but hopefully more reliably at large x , as predicted by models.

The dominance of FSI at $x = 1$ opens a new field of investigation. This feature can be advantageously used to study CT in few-body systems which should manifest as a function of Q^2 by a reduction of the cross section at large recoil momentum ($p_r > 400$ MeV/ c).

Finally, there are indications that the electromagnetic properties of nucleons are modified in the nuclear medium. The still on-going activity in this domain, as well on the analysis front as on the future experimental program, will confirm the status of these modifications.

Acknowledgements

I would like to thank the organizers of the XXIIrd International Workshop on Nuclear Theory for their invitation and warm hospitality at Rila Mountain.

This work was supported in part by the U.S. Department of Energy (DOE) contract DE-AC05-84ER40150 Modification No. M175 under which the Southern Universities Research Association (SURA) operates the Thomas Jefferson National Accelerator Facility, the National Science Foundation, the Italian Istituto Nazionale di Fisica Nucleare (INFN), the French Atomic Energy Commission and National Center of Scientific Research, and the Natural Science and Engineering Research Council of Canada.

References

- [1] S. Frullani and J. Mougey, *Adv. Nucl. Phys.* **14** (1984) 1.
- [2] J.J. Kelly, *Adv. Nucl. Phys.* **23** (1996) 75.
- [3] P. Ulmer *et al.*, *Phys. Rev. Lett.* **89** (2002) 062301.
- [4] M.M. Rvachev, F. Benmokhtar, E. Penel-Nottaris *et al.*, *nucl-ex/0409005*, (2004).
- [5] B. Reitz, Proc of the *International Workshop on Probing Nucleons and Nuclei with the $(e, e'p)$ reaction*, Edts. E. Voutier, J.-M. Laget, D. Higinbotham, Grenoble (France), 14-17 October 2003.
- [6] A. Afanasev *et al.*, *Hall A - 12 GeV upgrade: pre-conceptual design report*, Jefferson Laboratory, (2002).
- [7] J. Gao *et al.*, *Phys. Rev. Lett.* **84** (2000) 3265.

- [8] R.A. Niyazov, L.B. Weinstein *et al.*, *Phys. Rev. Lett.* **92** (2004) 052303.
- [9] F. Benmokhtar, M.M. Rvachev, E. Penel-Nottaris *et al.*, *nucl-ex/0408015*, (2004).
- [10] S. Strauch, S. Dieterich *et al.*, *Phys. Rev. Lett.* **91** (2003) 052301.
- [11] T. de Forest, *Nucl. Phys.* **A 392** (1983) 232.
- [12] J. Alcorn, *Nucl. Inst. Meth. Phys. Res.* **A 522** (2004) 294.
- [13] Jefferson Lab Experiment **E94-004**, M. Jones, P. Ulmer, spokespeople, (1994).
- [14] J.-M. Laget, *nucl-th/0407072*, (2004).
- [15] Jefferson Lab Experiment **E89-044**, M. Epstein, A. Saha, E. Voutier, spokespeople, (1989).
- [16] E. Jans *et al.*, *Phys. Rev. Lett.* **49** (1982) 974.
- [17] R. Florizone *et al.*, *Phys. Rev. Lett.* **83** (1999) 2308.
- [18] A. Kievsky, E. Pace, G. Salme, M. Viviani, *Phys. Rev.* **C 56** (1997) 64.
- [19] J.-M. Laget, *Few Body Syst. Supp.* **15** (2003) 171.
- [20] C. Cioffi degli Atti and L. Kaptari, *nucl-th/0407024*, (2004).
- [21] J. Udias and J.R. Vignote, Cont. to the *XXIIIrd International Workshop on Nuclear Theory*, Rila Mountain (Bulgaria) 14-19 June, 2004.
- [22] M. Mazouz, Diploma Dissertation, Ecole Nationale Supérieure de Physique, Grenoble (France), 2003.
- [23] M. Rvachev, Ph.D. Thesis, Massachusetts Institute of Technology, Cambridge (MS, USA), 2003.
- [24] Jefferson Lab Experiment **E97-111**, J. Mitchell, B. Reitz, J. Templon, spokespeople, (1997).
- [25] S. Tadokoro, T. Katayama, Y. Akaishi, and H. Tanaka, *Prog. Theor. Phys.* **78** (1987) 732.
- [26] J.J van Leeuwe *et al.*, *Phys. Rev. Lett.* **80** (1998) 2543.
- [27] E. Penel-Nottaris, Doctorat Thesis, Université Joseph Fourier, Grenoble (France), 2004.
- [28] Jefferson Lab Experiment **E01-020**, W. Boeglin, M. Jones, A. Klein, J. Mitchell, P. Ulmer, E. Voutier, spokespeople, (2001).
- [29] W. Boeglin, Proc of the *International Workshop on Probing Nucleons and Nuclei with the (e, e'p) reaction*, Edts. E. Voutier, J.-M. Laget, D. Higinbotham, Grenoble (France), 14-17 October 2003.

- [30] A. Bianconi, S. Jeschonnek, N.N. Nikolaev and B.G. Zakharov, *Phys. Rev. C* **53** (1996) 576.
- [31] L.L. Frankfurt, M.M. Sargsian and M.L. Strikman, *Phys. Rev. C* **56** (1997) 1124.
- [32] E. Voutier *et al.*, Proc. of the *Second ELFE Workshop on Hadronic Physics*, Saint-Malo (France), Edts. N. d’Hose, B. Frois, P.A.M. Guichon, B. Pire and J. van de Wiele, DAPNIA-SPhN-**96-35** (1996) 107.
- [33] J.-M. Laget, Proc. of the *CT97, Workshop on Color Transparency*, Edt. E. Voutier, Grenoble (France), 25-27 June 1997, (1998) 131.
- [34] T.G. O’Neill *et al.*, *Phys. Lett.* **87** (1995) 87.
- [35] D. Abbot *et al.*, *Phys. Rev. Lett.* **80** (1998) 5072.
- [36] K. Garrow, D. McKee *et al.*, *Phys. Rev. C* **66** (2002) 044613.
- [37] S. Gilad, W. Bertozzi, and Z.L. Zhou, *Nucl. Phys. A* **631** (1998) 276c.
- [38] J. Udias, J. Javier, E.M. de Guerra, A. Escuderos and J. Caballero, Proc. of the *Vth Workshop on Electromagnetic Induced Two-Hadron Emission*, Lund (Sweden], 2001; *nucl-th/0109077*, (2001).
- [39] Jefferson Lab Experiment **E89-003**, W. Bertozzi, K. Fissum, A. Saha, L. Weinstein, spokespeople, (1989).
- [40] J.J. Kelly, *Phys. Rev. C* **60** (1999) 044609.
- [41] J.M. Udias, J.A. Caballero, E. Moya de Guerra, J.E. Amaro and T.W. Donnelly, *Phys. Rev. Lett.* **84** (1999) 5451.
- [42] J.A. Caballero, Cont. to the *XXIIIrd International Workshop on Nuclear Theory*, Rila Mountain (Bulgaria) 14-19 June, 2004.
- [43] Jefferson Lab Experiment **E01-108**, K. Aniol, S. Gilad, D. Higinbotham, A. Saha, spokespeople, (2001).
- [44] C. Marchand *et al.*, *Phys. Rev. Lett.* **60** (1988) 1703.
- [45] F. Benmokhtar, Ph.D. Thesis, Rutgers, The State University of New Jersey, Piscataway (NJ, USA), 2004.
- [46] G. Onderwater *et al.*, *Phys. Rev. Lett.* **78** (1997) 4893.
- [47] G. Onderwater *et al.*, *Phys. Rev. Lett.* **81** (1998) 2213.
- [48] D.L. Groep *et al.*, *Phys. Rev. Lett.* **83** (1999) 5443.
- [49] P. Grabmayr, Cont. to the *XXIIIrd International Workshop on Nuclear Theory*, Rila Mountain (Bulgaria) 14-19 June, 2004.
- [50] Jefferson Lab Experiment **E89-027**, W. Bertozzi, W. Boeglin, L. Weinstein, spokespeople, (1989).

- [51] B. Mecking, *Nucl. Inst. Meth. Phys. Res. A* **503** (2003) 513.
- [52] P. Monaghan, Proc of the *International Workshop on Probing Nucleons and Nuclei with the (e, e'p) reaction*, Edts. E. Voutier, J.-M. Laget, D. Higinbotham, Grenoble (France), 14-17 October 2003.
- [53] Jefferson Lab Experiment **E01-105**, W. Bertozzi, E. Piassetzky, J.W. Watson, S. Wood, spokespeople, (2001).
- [54] A.I. Akhiezer, M.P. Rekalov *Sov. Jour. Part. Nucl.* **3** (1974) 274.
- [55] R.. Arnold, C. Carlson, F. Gross, *Phys. Rev. C* **23** (1981) 363.
- [56] M. Jones *et al.*, *Phys. Rev. Lett.* **84** (2000) 1398.
- [57] O. Gayou *et al.*, *Phys. Rev. Lett.* **88** (2002) 092301.
- [58] P.A.M. Guichon and M. Vanderhaeghen, *Phys. Rev. Lett.* **91** (2003) 142303.
- [59] S. Dieterich *et al.*, *Phys. Lett. B* **500** (2001) 47.
- [60] Jefferson Lab Experiment **E93-049**, R. Ent, P. Ulmer, spokespeople, (1993).
- [61] D.H. Lu, K. Tsushima, A.W. Thomas, A.G. Williams and K. Saito, *Phys. Rev. C* **60** (1999) 068201.
- [62] Jefferson Lab Experiment **E03-104**, R. Ent, R. Ransome, S. Strauch, P. Ulmer, spokespeople, (2003).